TECHNICAL MEMORANDUMS

NATIONAL ADVISORY COMMITTEE FOR AERONAUTICS

No. 824

THE PHOTOELASTIC INVESTIGATION OF THREE-DIMENSIONAL STRESS AND STRAIN CONDITIONS

By G. Oppel

Forschung auf dem Gebiete des Ingenieurwesens
Vol. VII, No. 5, September-October 1936

Washington
April 1937

NATIONAL ADVISORY COMMITTEE FOR AERONAUTICS

TECHNICAL MEMORANDUM NO. 824

THE PHOTOELASTIC INVESTIGATION OF THREE-DIMENSIONAL STRESS AND STRAIN CONDITIONS*

By G. Oppel

SUMMARY

The present report contains the description and typical application of two photoelastic methods which are suitable for the study of stress and strain conditions in three dimensions, namely: the fixation method and the immersion method.

The former can be used in nearly all cases of static loading. It depends upon the possibility of transforming purely elastic into permanent deformations and gives an accurate picture of the stress and strain conditions.

The immersion method, in many cases, affords a good insight into such conditions under static and dynamic loading. It is also applicable to problems dealing with the tracing back of a dynamically produced stress condition to a static stress condition of the same type.

I. OPTICAL PRINCIPLES

Under certain conditions light of the same wave length travels through a transparent substance (such as stress-free glass or synthetic resin) with uniform velocity.

According to Huygens' undulatory theory of light (reference 1) with the all-penetrating luminiferous ether as carrier of the waves, every point in the ether acted upon by the light becomes the source of new light waves. In transparent substances with nondirectional optical properties the new light waves are spherical.

---

*"Polarisationsoptische Untersuchung räumlicher Spannungs- und Dehnungszustände." Forschung auf dem Gebiete des Ingenieurwesens, vol. VII, no. 5, September-October, 1936, pp. 240-248.

But such substances may lose this property on becoming deformed. The propagation of light in a small particle of the substance then resembles the propagation of light in a crystal.

For example: Glass which is optically isotropic before deformation, manifests under unidirectional stress the optical property of a uniaxial crystal (reference 2). Every point of the ether in the substance acted upon by the light becomes the simultaneous source of two light waves - one having the shape of a sphere, the other that of the surface of an ellipsoid of revolution. For any direction of rays through the point of origin of these light waves there are with one exception, two rays of unequal velocity. The light of each ray vibrates in only one plane and perpendicular to the direction of the rays. The planes of vibration of the two rays of one direction are at right angles to each other. One single ray velocity exists only in the direction through the point of origin of the light waves and the two points of contact of the wave surfaces. This particular direction is called the optic axis.

In general the propagation of light in a small arbitrarily deformed particle of transparent matter resembles the propagation of light in an optically biaxial crystal (reference 2).

Every point of the ether in the substance which is acted upon by the light becomes the source of light waves with a two-sheeted wave surface of the fourth order.

By the use of a different presentation this surface can be replaced by a more simple one, the so-called Fresnel ellipsoid (fig. 1).

The two ray velocities belonging to each ray direction S and their corresponding planes of vibration are obtained by passing a plane E perpendicular to S through the center P of the ellipsoid. The half-lengths of the principal axes L_1 and L_2 of the elliptical section give the two ray velocities v_1 and v_2. The direction of the principal axis L_1 (L_2) of this elliptical section together with direction S define the plane of vibration of the light ray v_1 (v_2).

The half-lengths of the principal axes of Fresnel's ellipsoid correspond to the so-called three principal light velocities v_I, v_{II}, and v_{III}. Two planes can be

passed through the center of the triaxial ellipsoid whose sections with the ellipsoidal surface are circles. The directions of these two planes are called the optic axes. There is only one ray velocity for the axes. The axes lie in the plane through the maximum and minimum principal velocity of the light.

In the case of the optically uniaxial crystal, the light velocity and vibratory relations of the unidirectional condition of concentrated stress just considered can be represented by Fresnel's ellipsoid with two equal principal axes. The optic behavior of a small homogeneously deformed particle is determined if Fresnel's ellipsoid, with the directions of its principal axes are known.

The numerous photoelastic studies available on two-dimensional stresses in the common materials (glass, trolon, bakelite) show that the directions of the principal stress and strain, in the range of purely elastic behavior of the material coincide with the directions of the principal light velocities of Fresnel's ellipsoid.

Figure 1 shows that a light ray in the direction of the principal light velocity v_{III} penetrates the substance at velocity v_{II} if the plane of vibration of the ray is coincident with the plane through v_{III} and v_{II}. According to the data for the two-dimensional stress condition the difference of velocity v_{II} in the deformed and of velocity v_o in the nondeformed particle is proportional to the principal axial stress σ_I, which is perpendicular to the plane of vibration of the light ray:

$$v_{II} - v_o = C \sigma_I$$

(C = a constant for the material, determined by a calibration test.)

Brewster stated this law in similar form in 1816 for the conditions of unidirectional stress (references 3, 4, and 5). For small deformations the relation between stress and strain follows Hooke's law.

If the effect on the light of the proximity of a particle can be shut out - the deformations and the optical properties of the neighborhood are different, in general - the shape and the directions of the principal axes of Fresnel's ellipsoid for a small, homogeneously deformed

particle of matter can be defined by the conventional methods employed in crystal optics (by Jamin or Mach's interferometer, for example).

II. METHOD OF FIXATION

1. Principle of the Method

With the aid of a new phenomenon in the behavior of materials, it is possible to determine the optical properties of heterogeneously deformed particles in a body consisting of doubly refracting material. This behavior is strikingly manifested in synthetic resin products such as trolon and bakelite.

For example, if trolon is heated to 80° C., and at that temperature subjected to purely elastic deformation, and subsequently cooled without change in the deformation, the stresses are removed. The condition of elastic deformation becomes fixed.

Complete fixation of the previously elastic condition occurs as soon as the temperature drops below a threshold value (about 35° C. for trolon); softening takes place as soon as the temperature rises above the threshold value. At 20° C., for instance, we find that the purely elastic deformations - at 80° C. - have become permanent deformations. But the optical anisotropy (directional optical property) is preserved with the deformations after the stresses have gone.

Every particle of the deformed body reacts to light like a crystal. Pieces may be cut out of the material, that has been relieved of stress by the fixation, without disturbing their reaction to light. Their optical properties, strain condition, and the stress condition that was effective at 80° C., can be determined by the method described.

The author uses the apparatus shown in figure 2 for stress analysis with linearly and circularly polarized parallel light and with crossed polarizers. The interference patterns for monochromatic circularly polarized light show lines of equal illumination, corresponding to the lines of equal path difference which the two vibrations along the direction S with velocities v_1 and v_2

(fig. 1) have undergone by traversing the homogeneously deformed particles.

2. Example of Application

As an example of the application of the fixation method, the pressure of a sphere on a block will be discussed.

a) Determination of the condition of stress.- Two blocks of trolon (2.9 x 4.7 x 4.7 cm and 4.7 x 4.5 x 3.0 cm) in hot water at 80° C. were each subjected to a pressure of 14 kilograms by means of a 5-centimeter diameter steel ball. After the fixation of the elastic deformations by cooling to room temperature, one block was sliced into sections parallel to the load axis (fig. 3) (and the other block into sections at right angles to this axis (fig. 10)) - the slices being about 2 millimeters in thickness - which were then studied with the apparatus (fig. 2).*

If the ray direction coincides with a principal normal stress or, correspondingly, with one of the principal light velocities, for instance, with v_{III}, figure 1, the difference of path δ between the sinusoidal light vibrations for a ray path s is linearly proportional to the velocity difference $v_{II} - v_I$ of the two rays belonging to ray direction III.

Let ω be the phase angle velocity in radians per second ($\omega = 2\pi n$, n = frequency)

λ, wave length of light

t, time

v_o, velocity of light in undeformed material

then we have:

$$\delta = \omega (t_I - t_{II}); \quad t_I = s/v_I, \quad t_{II} = s/v_{II};$$

$$\delta = \omega \frac{v_{II} - v_I}{v_I \, v_{II}} \, s \approx \frac{\omega}{v_o^2} (v_{II} - v_I) \, s \qquad (1)$$

---

* The slices, becoming rough and opaque by cutting, were immersed in a fluid having the same refractive index.

The changes in the refractive index, due to the deformation being slight, we may put $v_I\, v_{II} = v_o^2$ in equation (1). Since $\omega\lambda = 2\pi v_o$ and $v_{II} - v_o = C\,\sigma_I$, we have:

$$\delta = 2\pi \frac{C}{\lambda\, v_o} (\sigma_I - \sigma_{II})\, s;$$

$$\frac{\delta}{2\pi} = n = \frac{k}{2} (\sigma_I - \sigma_{II})\, s = k\, \tau_{I\ II}\, s \qquad (2)$$

Here n is the order of the difference in path δ. $\tau_{I\ II}$ is one of the three principal shearing stresses in the stress condition of a small particle of the material. The photoelastic characteristic coefficient k of the material was found in a fixation test at 80° C. with a bending specimen of trolon to be $k \approx 3.7$ cm/kg (at 20° C: $k \approx 0.18$ cm/kg) for light of wave length $\lambda \approx 5500$ Å.

From equation (2) it follows: If the direction of the rays coincides with a direction of principal normal stress, the path difference for a ray path s in homogenously deformed material is linearly proportional to the amount of the difference of the other two principal normal stresses - small deformations being assumed.

Under the vertical pressure of a ball on the flat surface of a large block, two principal normal stress directions in every particle fall, for reasons of symmetry, in the planes through the axis of symmetry. The third principal normal stress direction is at right angles to the other planes. This also holds good at the faces of a sufficiently thin section which contains the load axis and is bounded by planes parallel to the load axis. Observing such a section in the apparatus under monochromatic circularly polarized light and with the incident rays perpendicular to the plane of the section, the lines of equal illumination represent lines of equal principal shearing stress because the ray direction in every point of this section coincides with a principal light velocity (fig. 4). Similarly, the lines of equal illumination in the interference patterns for sections 2, 3, and 4 can be interpreted approximately as lines of equal principal shear stress, because the sections still lie under the common contact surface between steel ball and block (figs. 5, 6, and 7). The reduction in the number of zones is indicative of the decrease in the stresses. The interference fringes, figure 8, after the cross cut through section 1,

show the altogether minor effect of the mechanical division on the optical behavior of the material relieved of stress by the process of fixation.

The stresses in the center section are compared with the stresses which L. Föppl derived along the axis of symmetry by computation.

Since Föppl's solution extends H. Hertz's (reference 7) theory of hardness, we shall state some important conclusions and compare them with the experimental results.

b) Comparison of the experimental test results of Hertz's (reference 7) and Föppl's (reference 6) solutions, according to the theory of elasticity.- Tests of the elastic behavior of trolon at 80° C., gave the following values:

Modulus of elasticity $E \approx 130$ kg/cm² (tensile test) (at 20° C: $E \approx 25{,}000$ kg/cm²)

Poisson's ratio $m \approx 2.8$ (compression test)

Shear modulus $G = \frac{m}{2(m+1)} E \approx 48$ kg/cm²

Proportional limit ≈ 18 kg/cm² (tensile test) (at 20° C: ≈ 100 kg/cm²)

At constant temperature (80° C.) these values may change with the duration of the heat treatment. The reason for this change probably follows from the observation that prolonged exposure to high temperature is followed by the conversion of solid constituents of the material into gaseous ones.

TABLE I

Radius a of Surface of Contact

Test data	Theoretical solution according to H. Hertz
$a = 5.6$ mm	$a = \sqrt[3]{3P\,r\left(\frac{m-1}{8mG}_{\text{steel}} + \frac{m-1}{8mG}_{\text{trolon}}\right)}$ $\approx \sqrt[3]{3P\,r\,\frac{m-1}{8mG}_{\text{trolon}}} \approx 5.6$ mm

TABLE II

Mean Compressive Stress p_m on Surface of Contact

Test data	Theoretical solution
$p_m = P/\pi a^2 =$ $= 14.2$ kg/cm^2	$p_m = 14.2$ kg/cm^2 Maximum stress $p_o =$ $= 1.5\ p_m$ $= 21.3$ kg/cm^2

If a sphere of radius $r = 2.5$ cm exerts a pressure $P = 14$ kg on the surface of contact between sphere and block, there are obtained values as found in tables I to III.

According to table III, the experimental values for the principal shear stresses τ_I and τ_{II} along the axis of symmetry, are in good agreement with the theoretical solutions, except for the area right next to the surface of contact.

An even better agreement is obtained by drawing a curve through the experimental points in figure 9 and then shifting the curve in the Z direction parallel to the axis of symmetry by 7 percent of the radius of the contact surface.

The position of the experimental points plotted in figure 9 was determined from the fringe ($z = 0$). The delineation of the fringe for a trolon specimen is subject to a disturbance* of the order of magnitude of 7 percent of the radius of the surface of contact if the rays are, as in the investigation, parallel to the bounding planes of the section. The fringes of figure 12 manifest this disturbance clearly. This is probably the principal cause of the discrepancy between the theoretical and the experimental values.

*Subsequently it was determined that the disturbances are not perceptible immediately after slicing, but have developed within a few hours to such an extent that the accuracy of measurement may be impaired. The effect is also present in material which does not refract light, if the section is not fresh. The measurements near the edge are the more accurate, the fresher the cut is at the time of measurement.

TABLE III

Principal Shear Stresses (cf. figs. 4 and 9)

Test data					Theoretical solution (L. Föppl)			
According to equation (2): $\tau = n/ks$; thickness of section $s = 0.21$ cm, $k = 3.7$ cm/kg. $\tau_I = \tau_{II} = \tau = n\ 1.29$ kg/cm^2					(formulas in fig. 9)			
$\frac{z}{a}$	n	Principal shear stress τ kg/cm^2	.... p_m	.... p_o	$\frac{z}{a}$	Principal shear stress τ .... p_o	.... p_m	kg/cm^2
0.03	3	3.9	0.27	0.18	0.03	0.11	0.17	2.3
.08	3.5	4.5	.32	.21	.08	.15	.23	3.3
.15	4	5.2	.36	.24	.15	.20	.31	4.4
.22	4.5	5.8	.41	.27	.22	.24	.36	5.2
.43	5	6.5	.45	.30	.43	.29	.44	6.2
.62	4.5	5.8	.41	.27	.62	.29	.44	6.2
.77	4	5.2	.36	.24	.77	.27	.41	5.8
.95	3.5	4.5	.32	.21	.95	.24	.36	5.1
1.15	3	3.0	.27	.18	1.15	.20	.31	4.4
1.37	2.5	3.2	.23	.15	1.37	.17	.25	3.6
1.69	2	2.6	.18	.12	1.69	.13	.20	2.8
2.25	1.5	1.9	.14	.09	2.25	.08	.12	1.8
3.06	1	1.3	.09	.06	3.06	.05	.07	1.0

In order to show by experiment that the third principal shear stress τ_{III} for the axis of symmetry is equal to zero, one block was sliced perpendicular to the load axis as illustrated in figure 10.

On a small particle through which the axis of symmetry passes (fig. 9), the compressive stresses perpendicular to this axis, are everywhere the same. For this reason there can be no path difference through such a particle if the section is analyzed under light falling at right angles to the plane of the section and using the apparatus described.

The lines of equal path difference are circles whose centers coincide with the axis of symmetry (figs. 11 to 13). The path difference for the center is equal to zero, rises to a maximum radially, and drops to zero toward the outer edge of the block.

In linearly polarized light the isochromatic patterns show a superimposed cross of dark lines (fig. 14). These dark lines are called "isogyres." The isogyre indicates all points for which the principal axes of the elliptical section of Fresnel's ellipsoid coincide with the vibration planes of the crossed polarizers.

III. THE METHOD OF IMMERSION

1. Principle of the Method

The refractive index of the solid, transparent substances especially suitable for photoelastic studies (such as glass, trolon, and bakelite) changes very little as the result of deformation. For photoelastic glass, this change amounts, at the most, to about 10^{-4}; for bakelite and trolon, about 1.5×10^{-3}. Consequently, the deflection of the rays, even in a heterogeneously deformed substance, is not very great. The passage of the light through the substance is almost rectilinear. But on entering transparent substances, as on emerging from them, the light can be materially deflected if the normals to the boundary surfaces are at an angle to the light rays and the index of refraction of the doubly refracting material is markedly different from that of the surrounding material - air glass, for instance. If the doubly refracting material is placed in a medium of equal refractive index, the ray experiences no

deflection when passing from this medium to the material or vice versa, no matter what the boundary of the deformed doubly refracting material. Fluids are best suited as mediums of equal refractive index. Figure 15 illustrates the refraction of light at a simple boundary between two mediums of unequal refractive indices n_1 and n_2. A transparent body of any form immersed in a fluid of equal refractive index can be analyzed under parallel polarized light with the apparatus (fig. 2). The interference patterns that appear under illumination have, in general, a very complicated relationship with the stress conditions. The path difference of the rays is induced by deformation conditions and stress conditions which vary along the path of the ray, both as regards their principal directions and their type. But even so, the relationship of the interference patterns can generally be adequately interpreted if the principal directions for the ray path in the heterogeneously deformed body are approximately constant, or if the directions of the two principal normal stresses with the largest difference in magnitude (largest principal shear stress) remains nearly constant along the path of the ray.

Two technically important examples of these cases are given in the following. The examination of the stress condition was accomplished without destroying the specimen.

Beginnings of the immersion method may be found in the work of Z. Tuzi, who in 1927 investigated a prismatic bending specimen of trapezoidal section in a fluid of equal refractive index (reference 8).

2. Examples of Application

a) Bending of bars of constant and variable circular cross section.- The bending and illumination of bars with constant and variable circular cross sections affords examples of the case in which the principal stresses and principal strains along the ray path remain almost in the same direction.

Figures 16 to 19 show such bars immersed in fluids of equal refractive index (mixtures of carbon disulphide and turpentine) and analyzed under parallel circularly polarized light with the apparatus of figure 2. The ray path was perpendicular to the plane of bending. The lines of equal illumination are lines of equal path difference.

The interference fringes for the notched bar (figs.

17 to 19), show that the interference pattern for the minimum cross section differs from that for the cylindrical part of the bar. These phenomena point to the well-known fact that under the same loading the stresses and strains present in the minimum section differ from those in a cylindrical bar of the same diameter.

The points of maximum path difference - they appear as sources of the zones as the load is increased - lie, in the smallest cross section, relatively closer at the bottom of the notch than in the cylindrical part of the bar at the outer edge. This shifting of maximum values indicates the increase in stress in the notch from the combined effects of form and load.

Figure 20 shows the trolon specimen partly in a medium of equal refractive index (right side) and partly in air (left side). The picture illustrates the explanations of figure 15 and by comparison, illustrates the purpose and success of the immersion method. The darker portion of figure 20 shows the result of the illumination of the bar in air, the lighter portion with the visible interference bands, the result of using a medium of equal refractive index.

b) Pressure of a ball on a block.- If a block of transparent, doubly refractive material (glass, for instance) on which a sphere is being pressed is illuminated with circularly polarized light between parallel polarizers with the direction of the rays perpendicular to the load axis, interference fringes are produced as in figures 21 to 24. The path difference of the rays is brought about by deformation and stress conditions which vary along the ray path as to both their principal direction and their nature. A particle contributes its maximum share to the path difference on a path Δs if the incident rays are perpendicular to the plane through the maximum and minimum principal normal stresses. In our investigation this is the case for those particles which lie under the common contact surface between ball and block and near to the load axis. The stress condition of these particles discloses, moreover, the absolute maximum principal normal stress differences. For this reason, the illumination yields an interference pattern which gives approximately the difference of the principal normal stresses in a plane through the load axis.

The comparison of figures 21 to 23, with figures 4 to 7, shows the similarity of the interference fringes.

Translation by J. Vanier,
National Advisory Committee
for Aeronautics.

REFERENCES

1. Huygens, Chr.: Traité de la lumière. Leyden 1690. Deutsch: Ostwalds Klassiker Bd. 20 (1890).

2. Müller-Pouillet's Lehrbuch der Physik, Optik II. Hälfte, 1. Teil, Braunschweig, 1929.

3. Brewster, D.: On the Communication of the Structure of Doubly Refracting Crystals to Glass, Muriate of Soda, Fluor Spar, and Other Substances by Mechanical Compression and Dilatation. Phil. Trans. Roy. Soc., London, 1816, p. 156.

4. Coker, E. G., and Filon, L. N. G.: A Treatise on Photo-Elasticity. Cambridge, 1931.

5. Föppl, L. and Neuber, H.: Festigkeitslehre mittels Spannungsoptik. München, 1935.

6. Föppl, L.: Der Spannungszustand und die Anstrengung des Werkstoffes bei der Berührung zweier Körper. Forschg., Bd. 7 (1936) Nr. 5, S. 209 (dieses Heft).

7. Föppl, A. u. L.: Drang und Zwang, Bd. II, 2. Aufl. München und Berlin, 1928.

8. Tuzi, Z.: Photo-Elastic Study on a Specimen of Three Dimensional Form. Sci. Pap. Inst. Physic. chem: Res., Tokyo, Bd. 7 (1927) S. 97.

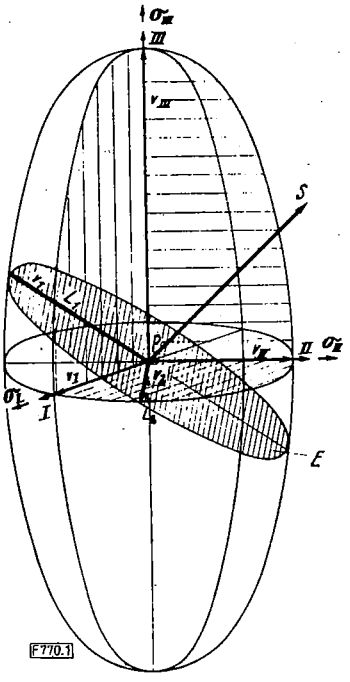

Figure 1.-Fresnel's ellipsoid. It characterizes the propagation of light in any small deformed particle of a transparent substance.

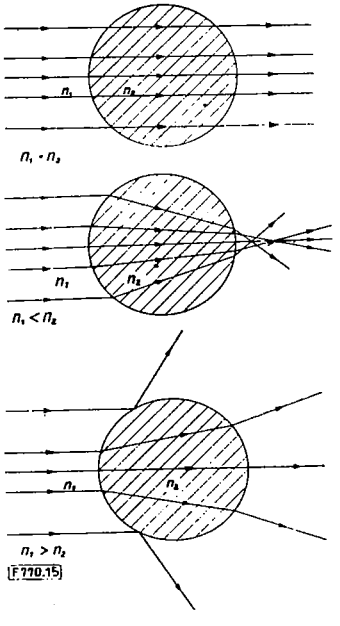

Figure 15.-Refraction of light at the boundary between two mediums having different refractive indexes n_1 and n_2 .

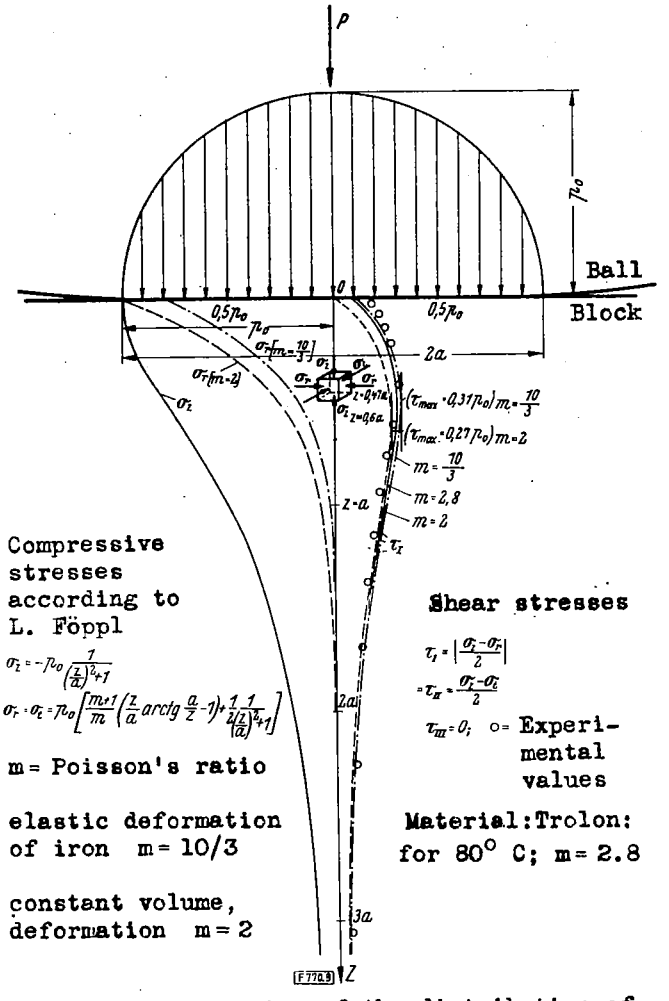

Figure 9.-Representation of the distribution of stress along the axis of symmetry. The experimental values of the principal shear stress τ from table III are compared with the theoretical solution by L. Föppl.

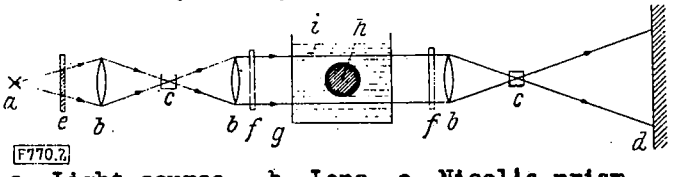

a, Light source b, Lens c, Nicol's prism
d, Screen or photographic plate
e, Green filter } $\lambda \approx 5500$ Å
f, Mica plate }
g, Glass box with plane parallel walls
h, Test specimen
i, Fluid (refractive index of fluid = refractive index of the test specimen.)

Figure 2.- Apparatus for the photo-elastic investigation of three dimensional stress and strain conditions.

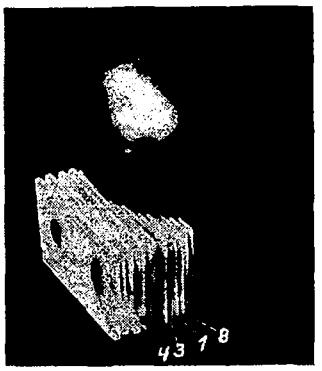

Figure 3.- Arrangement of slices(sections) parallel to the axis of pressure. Material: Trolon. The sections,about 2 mm thick were analyzed with the apparatus(Fig.2) to determine the stress distribution that was effective at 80°C.

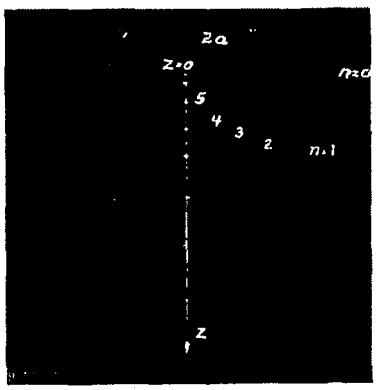

Figure 4.- Center section 1 through the block. The lines of equal illumination correspond to the lines of equal principal shear stress. Magnification:2.8, reduced to 2/3 size.

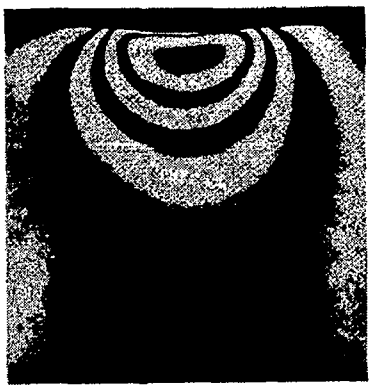

Figure 5.- Section 2 through the block magnification:2.8, reduced to 2/3 size.

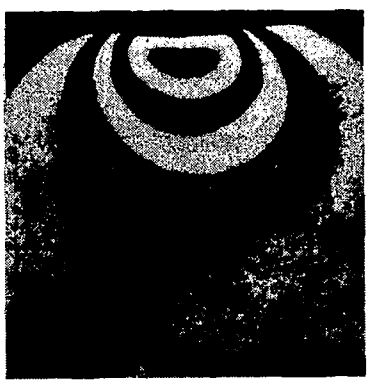

Figure 6.- Section 3 through the block magnification:2.8, reduced to 2/3 size.

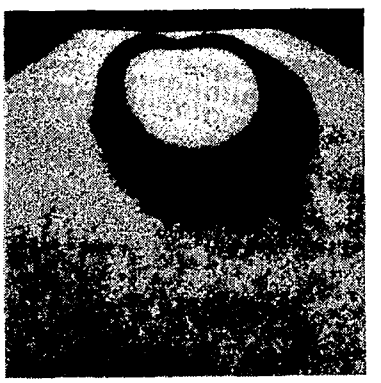

Figure 7.- Section 4 through the block magnification:2.8, reduced to 2/3 size.

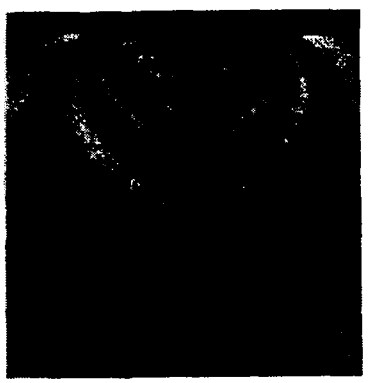

Figure 8.- A cross cut through the center section 1 magnification:2.8 , reduced to 2/3 size.

Figures 3-8.- Investigation of the stress distribution due to the pressure of a ball on a block by the fixation method.

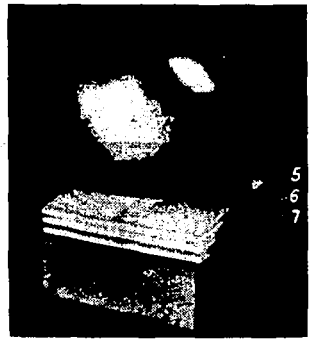

Figure 10.- Arrangement of slices(sections) at right angles to the load axis.

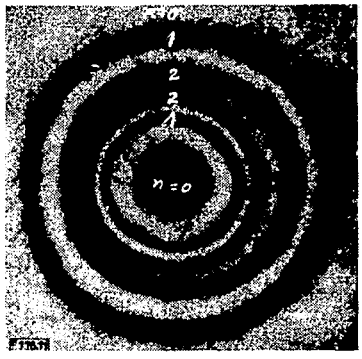

Figure 11.- Section 5 magnification:2.8, reduced to 2/3 size.

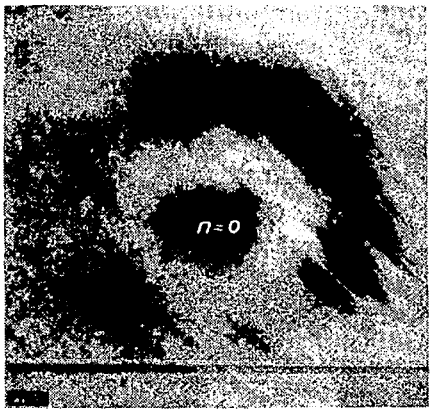

Figure 13.- Section 7 $z \simeq 2a$ Magnification:2.8, reduced to 2/3 size.

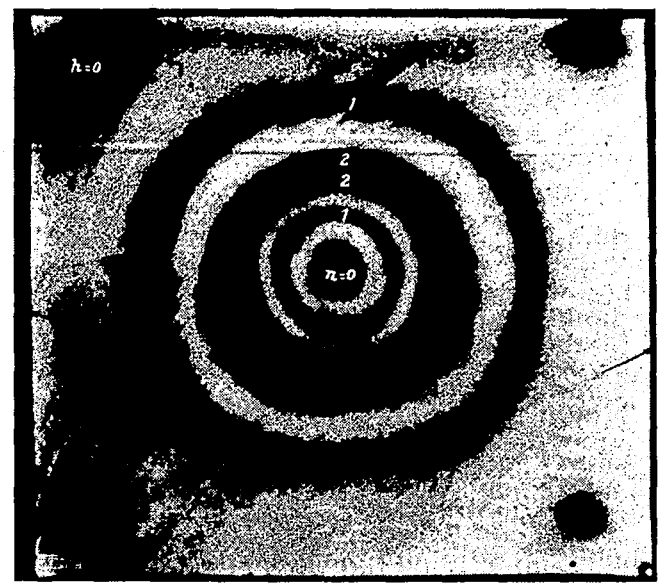

Figure 12.- Section 6, the deformation of the edge indicates distortion by which a discrepancy is caused between the theoretical and the experimental results. Magnification:2.8, reduced to 2/3 size.

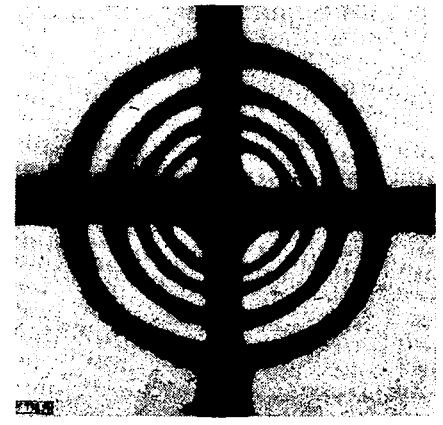

Figure 14.- Section 5 In linear polarized light a dark cross(Isogyre) appears superposed on the isochromatic pattern. Magnification:2.8 , reduced to 2/3 size.

Figures 10,11,12,13,14.- Investigation of the distribution of stresses produced by the pressure of a ball on a block using the method of fixation.

Figure 16.- Glass rod of uniform circular section loaded in bending, analyzed by the method of immersion. Magnification:2.8, reduced to 2/3 size.

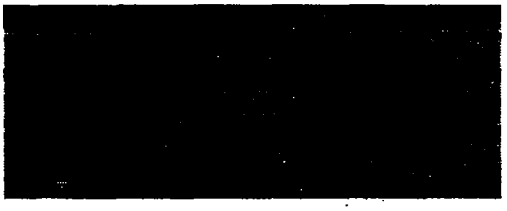

Fig. 17

Fig. 18

Fig. 19

Figures 17,18,19.- Notched Trolon bar of circular section loaded in bending, analyzed by the immersion method. The bending load increases from Fig.17 to Fig.19. Magnification:2.8, reduced to 2/3 size.

Figure 20.- Trolon bar partly in air(left) partly in a medium having the same refractive index(right).

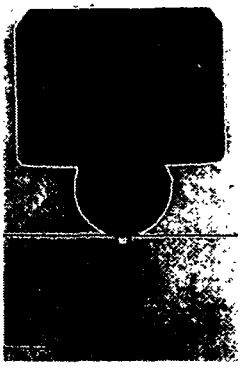

Fig. 21
P ≈ 5 kg

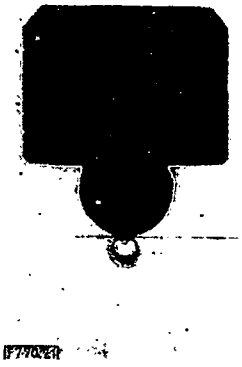

Fig. 22
P ≈ 10 kg

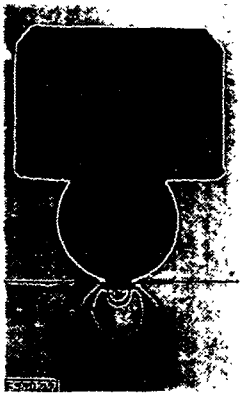

Fig. 23
P ≈ 40 kg

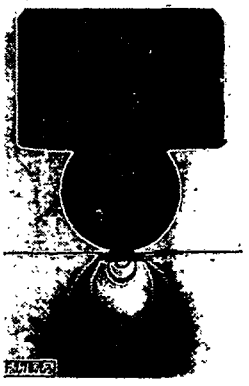

Fig. 24
P ≈ 60 kg

Figures 21,22, 23,24.- Pressure of a steel ball on a block of glass. Magnification:2.8, reduced to 3/4 size. Investigation by method of immersion.